Study of the hyperfine coupling constants (^{14}N and ^{1}H) of the NH_2 molecules in the $X\,^2B_1$ ground state and the $A\,^2A_1$ excited state

B. Engels, M. Perić,[a] W. Reuter, S. D. Peyerimhoff, and F. Grein[b]
Institut für Physikalische und Theoretische Chemie, Universität Bonn, Wegelerstrasse 12, D 5300 Bonn 1, Germany

(Received 12 November 1991; accepted 3 December 1991)

The hyperfine coupling constants (hfcc) A_{iso} and A_{ij} are calculated for the atoms of NH_2 in its two lowest-lying electronic states at various molecular geometries by means of the *ab initio* multireference configuration interaction method. The vibronically averaged values of the hfccs for the $K=0$ and 1 levels in $^{14}N\,^1H_2$ in the energy range up to 20 000 cm^{-1} are computed. Polarization effects which determine A_{iso} as well as a simple model to describe the dipolar hfccs are discussed. All results are in excellent agreement with experimental data.

I. INTRODUCTION

The amidogen radical NH_2 probably represents the most studied triatomic radical at the present time. The $A\,^2A_2$–$X\,^2B_1$ band spectrum has been the subject of intense experimental[1] and theoretical[2] investigations since it provides an excellent example of the Renner–Teller effect[3] for polyatomic molecules, with both participating electronic states correlating with the same $^2\Pi_u$ species in the linear nuclear arrangement. Accordingly, large effects related to the coupling of electronic (orbital) and vibrational angular momenta occur.

Various molecular constants such as rotational constants, centrifugal distortion constants, and spin rotational constants were measured by Cook, Curl, Hills, Brown, and co-workers[4] using the microwave optical double resonance (MODR) techniques. Also the hyperfine coupling constants (hfccs) composed of the isotropic part A_{iso} and the tensorial anisotropic part A_{ij} were studied for the lowest vibrational state of $X\,^2B_1$ and the vibrational states $v_2=4$, $K=0$ and $K=1$ ($v_1, v_3=0$) of the excited state $A\,^2A_1$.

The hfccs of the ground state $X\,^2B_1$ have been the subject of several theoretical studies.[5] Although none of the calculations consider effects arising from the nuclear motion, a comparison with experimental results is possible because such effects are expected to be small for the lowest vibrational level. Also, the perturbations due to the Renner–Teller effect are insignificant[2] for the lowest level of the $X\,^2B_1$ state. Deviations between experimental and theoretical data are found to be about 3–4 MHz. The hfcc of the isotopomers NHD and ND_2 were also calculated and it could be shown that the *ab initio* methods are able to generate reliable values not only for the diagonal, but also for the off-diagonal elements of A_{ij}.[5(f)]

While the influence of the nuclear motion and the Renner–Teller effect are small for the lowest vibrational level of $X\,^2B_1$ this cannot be expected for higher vibrational levels, such as $v_2=4$, $K=0$, and $K=1$ of the $A\,^2A_1$ state. An indication for the size of the effects is given by a calculation of Pöhlchen *et al.*[5(e)] They calculated the hfccs at the equilibrium geometry of $A\,^2A_1$ and found differences up to 60% to the experimental values. To dissolve the discrepancies between theory and experiment, in the present study the hfccs of both states are calculated and the results of an averaging of the isotropic and anisotropic parts of the hf operator over vibronic wave functions are presented. Furthermore, the influence of spin polarization effects on A_{iso} is discussed for both states.

II. TECHNICAL DETAILS

The isotropic and anisotropic hfccs describe the interaction between a nuclear spin **I** and the electron spin **S**. They are determined by the net unpaired electron-spin density at the nucleus and the spatial distribution of the electron-spin density. The former represents a scalar and is defined for a nucleus c as

$$a_{iso}^{c}=\frac{8}{3}\pi g_N g\beta_N\beta_e\frac{1}{S}\langle\Psi|\sum_{k=1}\delta(r_{ck})s_{zk}|\Psi\rangle,$$

where β_N and g_N are the nuclear magneton and nuclear g factor, respectively. The term g is the g value for the electrons in the free radical, while β_e is the Bohr magneton. In the present work, a value of 2.0 is used for g. The anisotropic part which is given by the dipole–dipole interaction between the nuclear spin **I** and the electron spin **S** represents a tensor. Its Cartesian components are defined in a molecule-fixed coordinate system as

$$A_{ij}^{c}=g_N g_e\beta_N\beta_e\frac{1}{S}\langle\Psi|\sum_{k=1}\left(\frac{3_{ij}-r^2\delta_{ij}}{r^5}\right)_{ck}2s_{zk}|\Psi\rangle,$$

with $i,j=x,y,z$; ck indicates that A_{ij} is formulated with respect to the center c. The anisotropic part is calculated within the principal axis of the tensor of inertia to facilitate a comparison to experimental data.[5(f)] Because the bent NH_2 molecule possesses C_{2v} symmetry, no off-diagonal electronic matrix elements have to be calculated for A_{iso} and the A_{ii}

[a] Permanent address: University of Belgrade, Faculty of Science, Institute of Physical Chemistry, Studentski trg 16, P.O. Box 550, 11001 Beograd, Yugoslavia.

[b] Permanent address: University of New Brunswick, Department of Chemistry, Bag Service Number 45222, Fredericton, N. B., Canada E3B 6E2.

 0021-9606/92/064526-10$06.00

components as it was necessary in a similar study of the C_2H radical.[6]

The atomic orbital (AO) basis set employed is given in Table I. All calculations are performed in the C_{2v} point group. The calculations are carried out in the standard manner, whereby the multireference configuration interaction (MRD-CI) truncation is made on the basis of the energy selection threshold T.[8] The dependence of the calculated hfccs on the quality of the CI wave function will be discussed in the next chapter in connection with the results. To obtain a faster convergence of the CI expansions, natural orbitals (NO) are employed for the $X\,^2B_1$ state. The calculations are performed at the equilibrium distances of the states in question, e.g., 1.935 a.u. for $X\,^2B_1$ and 1.87 a.u. for $A\,^2A_1$.

Since the aim of this study is to show with which accuracy the hfccs can be calculated by the *ab initio* method, we employ in the present treatment the potential curves published by Jungen, Hallin, and Merer, being derived by fitting the observed spectral data[2(c)] rather than the *ab initio* curves calculated in our laboratory[2(f),2(g)] in order to calculate the effect of vibrational motion. The reason for this choice is that the latter ones, suffering from inaccuracies inherent in the *ab initio* method ($\sim$0.1 eV), do not enable a quantitatively reliable description of local phenomena arising where neighboring levels belonging to different potential surfaces interact with each other.[10] Effects arising from the use of different bending potential energy curves will be given in connection with the results for the isotopomers NHD and ND_2.[9] The approach employed for the calculations of the vibronic wave function is described elsewhere.[10] The large amplitude bending vibrations are treated employing the semirigid bender Hamiltonian.[11] The vibronic wave functions are represented by expansions in the eigenfunctions of a two-dimensional harmonic oscillator. The vibronically averaged hfccs are calculated as integrals over these basis functions.

In the present paper, we employ the "bent" notation for the bending quantum number. The relation between v_2^{lin} and v_2^{bent} is $v_2^{\text{lin}} = 2\times v_2^{\text{bent}} + \Lambda(=1) + K$. K represents the quantum number conjugated to the component of the total angular momentum (excluding spin) along the axis a. Interaction due to the Renner–Teller effect arises only for $K>0$ levels.

III. RESULTS AND DISCUSSION

The results of the calculations of the hfccs of $X\,^2B_1$ are presented in Figs. 1–4. In Fig. 1, the calculations of $A_{\text{iso}}(^{14}\text{N})$ are summarized. The calculated value of $A_{\text{iso}}(^{14}\text{N})$ [at a configuration selection threshold of $T=0.3$ μhartree, which gives rise to 15 000–20 000 symmetry-adapted configuration state functions (SAFs) in the truncated CI] decreases from 44 MHz at $\Theta = 180°$ to 22 MHz at the equilibrium geometry $\Theta = 103.3°$. For the smallest angle considered in the present study ($\Theta = 40°$), a value of about 15 MHz was obtained. To study the dependency of $A_{\text{iso}}(^{14}\text{N})$ on the quality of the CI wave function, two calculations with different thresholds ($T=10.0$ μhartree giving rise to 2000–3000 SAFs and $T=0.3$ μhartree resulting in 15 000–20 000 SAFs) are performed for each geometry. The values given for the nearly equilibrium geometry $\Theta = 103°$ are taken from our previous paper.[5(f)]

It is seen that for all geometries, the value for $A_{\text{iso}}(^{14}\text{N})$ increases if the wave function is improved. The influence of the quality of the wave function on the value for hfccs decreases with decreasing angle, e.g., the difference in the values of A_{iso} calculated at $T=0.3$ and 10.0 μhartree is 10 MHz for $\Theta = 180°$, 5 MHz for $\Theta = 103°$, 2 MHz for $\Theta = 40°$. However, a reliable qualitative behavior of $A_{\text{iso}}(^{14}\text{N})$ as a function of Θ is already achieved with the wave function corresponding to the smaller CI space. Therefore, by using better wave functions, an overall shift in $A_{\text{iso}}(^{14}\text{N})$ can be expected. This can be seen from the calculations for $\Theta = 103°$. If T is lowered to 0.1 μhartree (treating 27 755 SAFs variationally), $A_{\text{iso}}(^{14}\text{N})$ rises by about 2 MHz (Fig. 1).

The calculated values of $A_{ij}(^{14}\text{N})$ are given in Fig. 2. Because a RHF calculation for A_{ij}, which is equivalent to the expectation value of the given operator calculated for the singly occupied $1b_1$ orbital, already gives 98% of the total value, no dependency on the quality of the wave function is noted. The very weak dependence of all tensor elements on Θ can be explained by the nature of the $1b_1$ orbital and that of the dipole–dipole operator. For all Θ values, the $1b_1$ orbital represents the p orbital of the nitrogen atom which lies perpendicular to the molecular plane. Due to this position which excludes interactions with the hydrogens, the shape of $1b_1$ does not change during the bending of the molecule. Furthermore, the relative position between the nitrogen nucleus and the density of the unpaired electron remains constant.

The hfcc of the hydrogen centers are summarized in Figs. 3 and 4. Due to symmetry reasons, the hfcc of both centers are equal to one another, except for the off-diagonal elements of the A_{ij} tensor which have the same magnitude, but differ in sign. From Fig. 3, it can be seen that starting from $\Theta = 180°$, the calculated value of $A_{\text{iso}}(^1\text{H})$ changes from -77 to -43 MHz at $\Theta = 40°$. Using a configuration selection threshold $T=0.3$ μhartree (15 000–20 000 SAFs), a value of -62 MHz is obtained for the equilibrium geometry ($\Theta = 103.3°$). The dependency on the quality of the CI wave function is similar to that found for $A_{\text{iso}}(^{14}\text{N})$. Therefore, from an improvement of the wave function, an overall shift to lower values of $A_{\text{iso}}(^1\text{H})$ is expected, e.g., about 2 MHz using $T=0.1$ μhartree (27 755 SAFs) instead of $T=0.3$ μhartree (17805 SAFs).

As for the nitrogen center, the values of the dipole tensor

TABLE I. The AO basis set employed in the present work.

Nitrogen	(13*s*8*p*) contracted to [8*s*5*p*][a,b]
	plus 2*d* (1.9/0.5)
	plus 1*f* (1.0)[c]
Hydrogen	(8*s*) contracted to [5*s*][a,b]
	plus 2*p* (1.4/0.25)

[a] Reference 7(a).
[b] Reference 7(b).
[c] Reference 7(c).

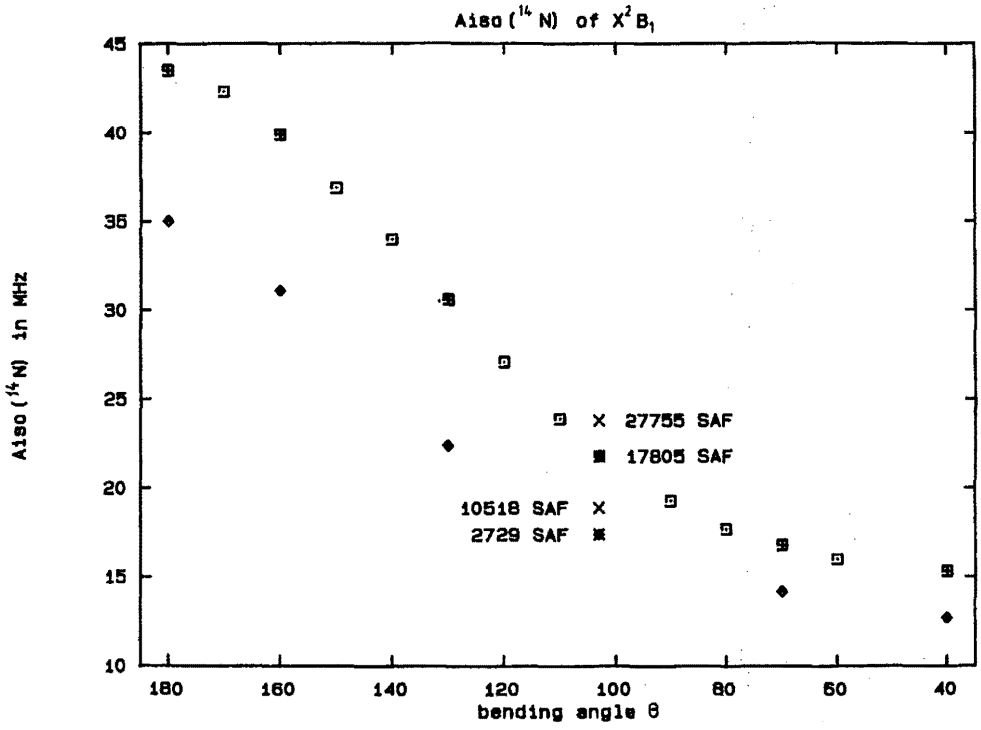

FIG. 1. The dependence of $A_{iso}(^{14}N)$ on the bending angle for the X^2B_1 ground state calculated at $R_{NH} = 1.93$ a.u. from different treatments. ◇ corresponds to CI expansions involving between 2000–3000 SAFs, + corresponds to CI expansions involving between 15 000–20 000 SAFs, □ are data points obtained by a spline fit. At $\Theta = 103°$, the calculated value is given for four different CI expansion lengths.

$A_{ij}(^1H)$ (Fig. 4) can be calculated reliably already with a restricted Hartree–Fock (RHF) wave function. However, contrary to $A_{ij}(^{14}N)$, the individual elements of $A_{ij}(^1H)$ possess a complicated functional dependency on the bending angle Θ. The behavior with respect to Θ is explained easily by expressing A_{ij} in spherical coordinates[12] and considering the relative position between the unpaired electron and the hydrogen center. The situation is sketched in Fig. 5. The changes in the components of A_{ij} by bending the molecule arise from the polar angle χ' which is nearly equal to one-half of the bending angle Θ. The qualitative behavior is described by a simple model in which the unpaired electron is located 1.2 a.u. above (and below) the nitrogen center, and further improvement is reached if it is shifted slightly towards the

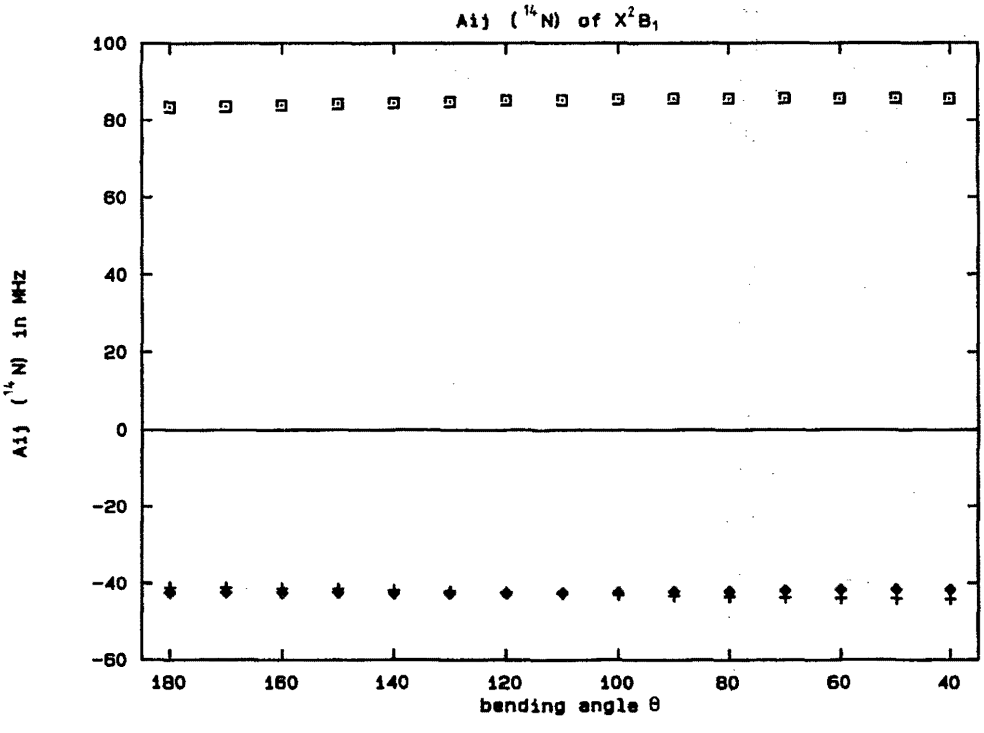

FIG. 2. The dependence of the components of $A_{ij}(^{14}N)$ on the bending angle for the X^2B_1 ground state calculated at $R_{NH} = 1.93$ a.u. The various points refer to the principal axes a, b, c of the inertial tensor ◇ $\equiv A_{aa}$, + $\equiv A_{bb}$, and □ $\equiv A_{cc}$.

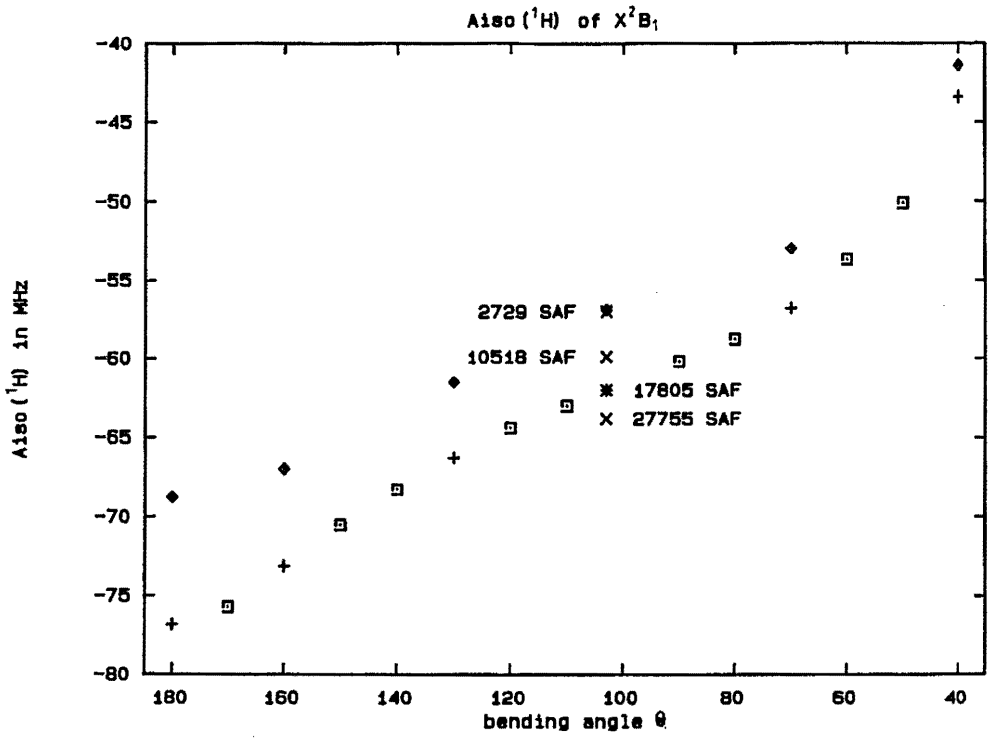

FIG. 3. The dependence of A_{iso} (^{1}H) on the bending angle for the X^2B_1 ground state calculated at $R_{NH} = 1.93$ a.u. obtained from different treatments. The explanation for the data points is the same as in Fig. 1.

hydrogen centers (by about 0.1 a.u.).[4(e),5(f)]

The results obtained for the excited $A\,^2A_1$ state are summarized in Figs. 6–9. For the calculated values of A_{iso} (^{14}N) (Fig. 6), a strong increase is found in going from a linear to a bent molecular geometry. The value of 104 MHz calculated at the equilibrium geometry ($\Theta = 144°$) shows excellent agreement with other theoretical studies.[5(e)] However, it is much smaller than the experimental value of the vibrational level $v_2 = 4$, $K = 0$ (155 MHz)[4(d)] which indicates the strong influence of the vibrational motion on the value of the $v_2 = 4$, $K = 0$ level. The dependency on Θ arises from the nature of the singly occupied $3a_1$ orbital. For $\Theta = 180°$, it represents a pure π orbital so that A_{iso} (^{14}N) is determined solely by polarization effects. By bending the NH_2 molecule,

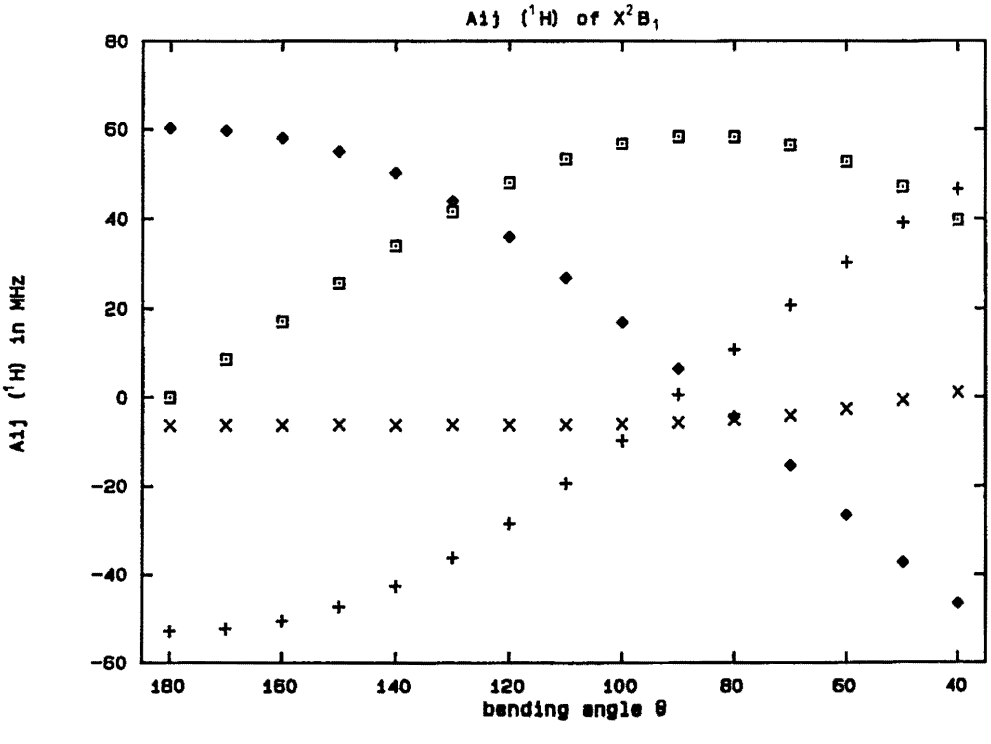

FIG. 4. The dependence of the components of A_{ij}(^{1}H) on the bending angle for the X^2B_1 ground state at $R_{NH} = 1.93$ a.u. The designation is similar to that of Fig. 2. $\Diamond \equiv A_{aa}$, $+ \equiv A_{bb}$, $\square \equiv A_{ab}$, and $\times \equiv A_{cc}$.

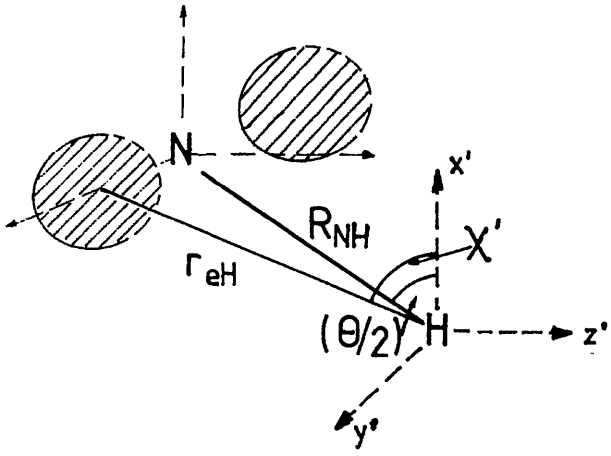

FIG. 5. A representation of parameters important for the calculation of $A_{ij}(^1H)$. (x', y', z') indicate the Cartesian coordinate system used for the calculation of $A_{ij}(^1H)$, χ' represents the polar angle. R_{NH} and Θ are the internuclear distance and the bending angle. r_{eH} is the distance between the hydrogen center and the unpaired electron. The shape of the $1b_1$ orbital is sketched by the shaded area.

the $3a_1$ orbital obtains more and more σ character from which a strong increase of the direct contribution from the $3a_1$ orbital to $A_{iso}(^{14}N)$ results. A detailed discussion of the individual effects will be given in the next section. From Fig. 6, it can be seen that the dependence of the value for A_{iso} on the quality of the wave function is small. By improving the wave function, an overall shift of 3–5 MHz is found. The values of $A_{ij}(^{14}N)$, given in Fig. 7, possess stronger dependencies on Θ than those found for $X\,^2B_1$. The variations arise from the change in the nature of the $3a_1$ orbital. Again, the calculated values are already given satisfactorily within the RHF approach. Like $A_{iso}(^{14}N)$, the value of $A_{iso}(^1H)$ increases strongly with decreasing angle Θ (Fig. 8). A change in sign is found near the equilibrium geometry. At the equilibrium geometry ($\Theta = 144°$), a value of 12 MHz is calculated. It agrees reasonably well with the value of 16 MHz given by Pöhlchen *et al.*[5(e)] The reasons for this behavior of $A_{iso}(^1H)$ are similar to those found for $A_{iso}(^{14}N)$. Contrary to $A_{iso}(^{14}N)$, the calculated value of $A_{iso}(^1H)$ decreases with improving wave function. The calculated functional dependency of the elements of the anisotropic tensor A_{ij} on the bending angle is given in Fig. 9. A simple model such as that given for $X\,^2B_1$ cannot be used for the $A\,^2A_1$ state because this model would not be able to incorporate the change in character of the singly occupied $3a_1$ orbital.

The hfccs obtained for the individual $K = 0$ and $K = 1$ rovibronic states are given in Figs. 10 and 11 and Tables II and III. While Figs. 10 and 11 contain a graphical representation of the results for $A_{iso}(^{14}N)$ and $A_{iso}(^1H)$, all calculated numbers are summarized in Tables II and III. The values of $A_{iso}(^{14}N)$ calculated for individual rovibronic states are summarized in Fig. 10. The values for $K = 0$ of the $X\,^2B_1$ state which include only averaging over the bending motion in this particular electronic state show only small dependencies on the vibrational quantum number. The reason for this behavior is twofold. First, for the $K = 0$ states, no mixing between the two electronic states $X\,^2B_1$ and $A\,^2A_1$ occurs and second, as discussed above, the dependency of $A_{iso}(^{14}N)$ on the bending angle Θ was found to be small for $X\,^2B_1$ (Fig. 1). For the $K = 0$ states of the electronically excited state $A\,^2A_1$ the large influence of the bending angle Θ on

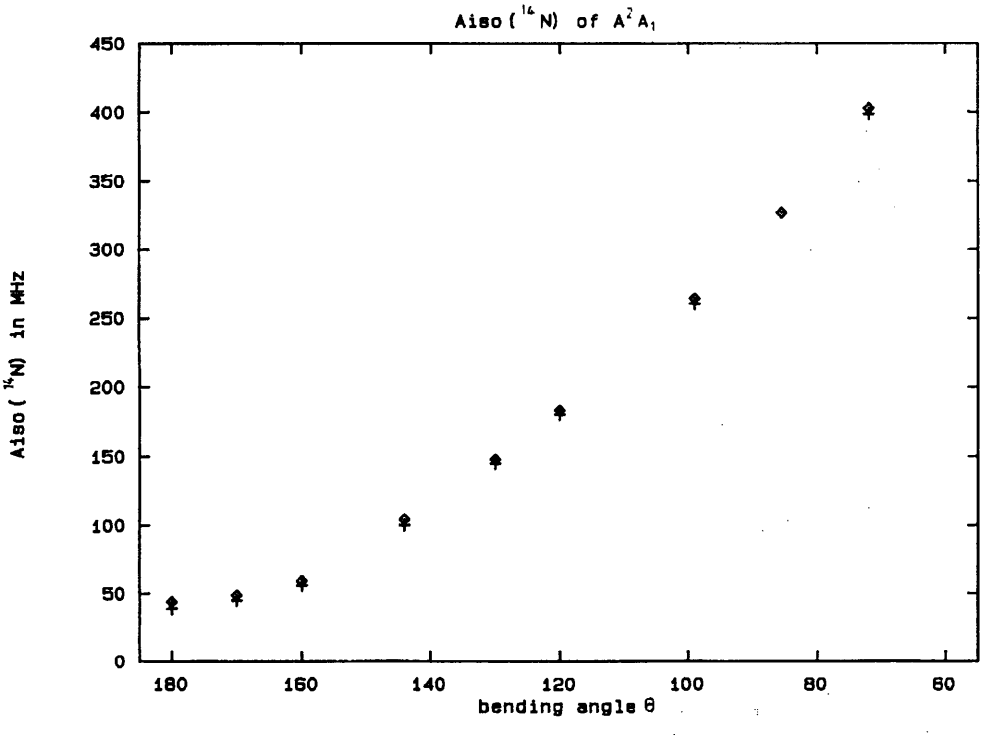

FIG. 6. The dependence of $A_{iso}(^{14}N)$ on the bending angle for the $A\,^2A_1$ state calculated at $R_{NH} = 1.87$ a.u. ◇ corresponds to CI expansion involving between 25 000 and 30 000 SAFs, + corresponds to CI expansion involving between 6000 and 10 000 SAFs.

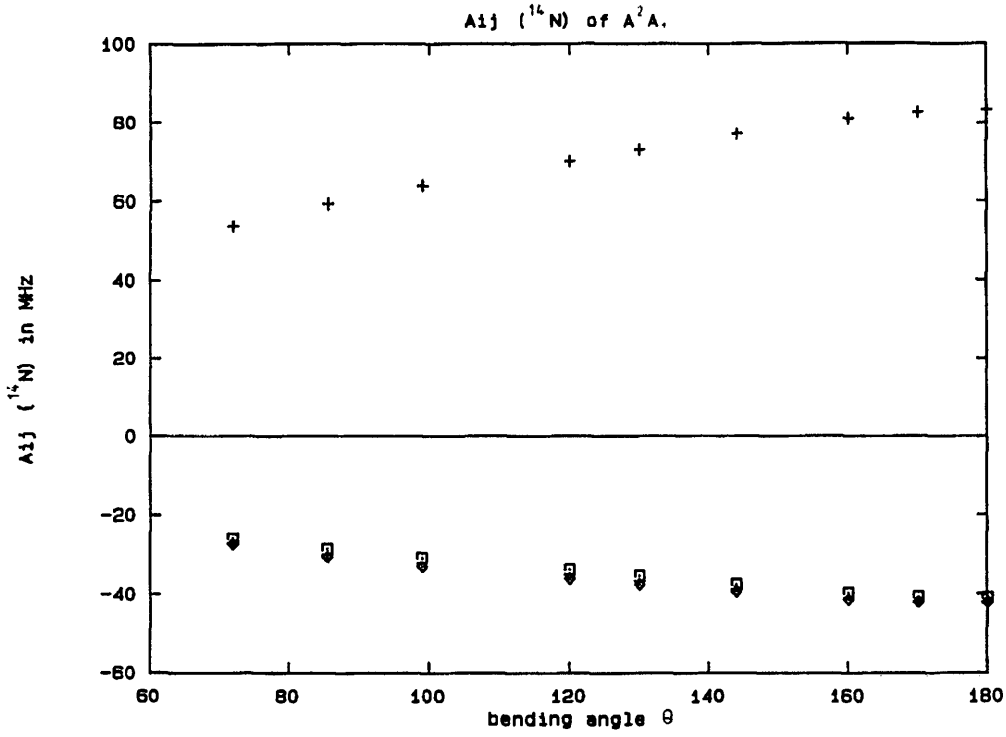

FIG. 7. The dependence of the components of $A_{ij}(^{14}N)$ on the bending angle for the $A\,^2A_1$ state calculated at $R_{NH} = 1.87$ a.u. The designations are equal to that of Fig. 2.

$A_{iso}(^{14}N)$ is reflected in the sharp increase of $A_{iso}(^{14}N)$ as a function of the increasing vibrational quantum number v_2.

In Fig. 10, experimentally known $A_{iso}(^{14}N)$ values of the NH_2 molecule are also given. The experimental value[4(a)-4(c)] of $A_{iso}(^{14}N)$ for the lowest vibrational level of the electronic ground state $X\,^2B_1$ is about 5 MHz higher than the calculated value given by the present work. The reason for the difference between theory and experiment lies in the dependency of the calculated value on the quality of the CI wave function (Fig. 1). Because, as discussed above, the relative behavior of $A_{iso}(^{14}N)$ with respect to the bending angle Θ is already obtained with smaller CI expansions, we expect that all calculated $A_{iso}(^{14}N)$ for $K = 0$ states of $X\,^2B_1$ have to be shifted higher by about 5 MHz in order to compare

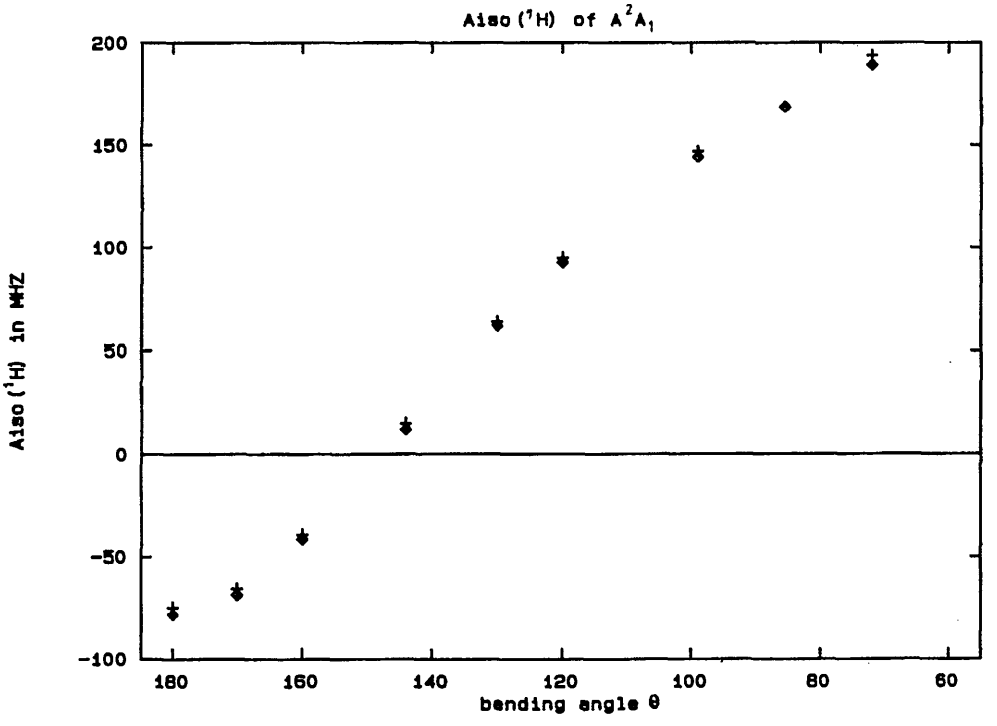

FIG. 8. The dependence of $A_{iso}(^1H)$ on the bending angle for the $A\,^2A_1$ state calculated at $R_{NH} = 1.87$ a.u. obtained for different treatment. The explanation for the data points is the same as in Fig. 6.

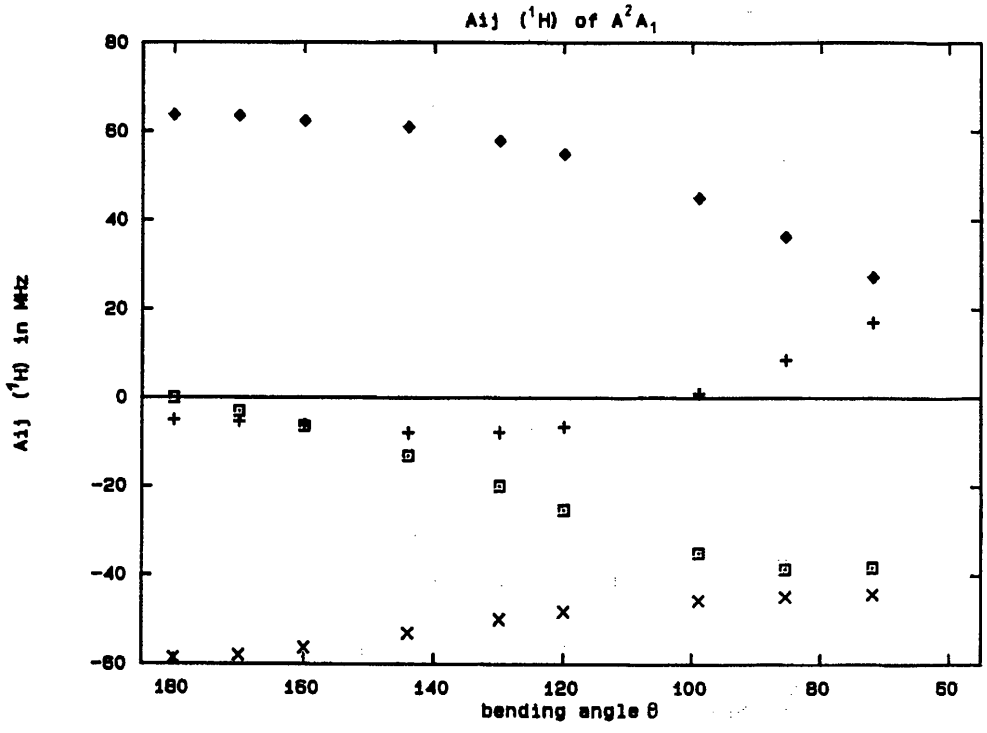

FIG. 9. The dependence of the components of $A_{ij}(^1\mathrm{H})$ on the bending angle for the $A\,^2A_1$ state calculated at $R_{NH} = 1.87$ a.u. The designation is equal to Fig. 4.

with experimental results. For similar reasons (Fig. 6), the calculated values of the $K = 0$ states of $A\,^2A_1$ are also expected to lie too low. However, part of the deviation between experiment and theory found for the $v_2 = 4$, $K = 0$ level (155 vs 148 MHz) has to be attributed to uncertainties in the experimental data[4(d)] (see Table II).

While $K = 0$ levels are attributed unambiguously to one electronic state, eigenfunctions of $K = 1$ involve both electronic states coupled via the Renner–Teller effect. Because the isotropic hfcc of both electronic states differs considerably, the amount of mixing found for a given vibronic state should be reflected in the averaged values of A_{iso}. In Fig. 10, $A_{iso}(^{14}\mathrm{N})$ of vibrational states possessing mainly $X\,^2B_1$ character are indicated by (+) and those possessing mainly $A\,^2A_2$ character by (×). Vibronic states below 10 000 cm^{-1} possess practically only $X\,^2B_1$ character because the Ren-

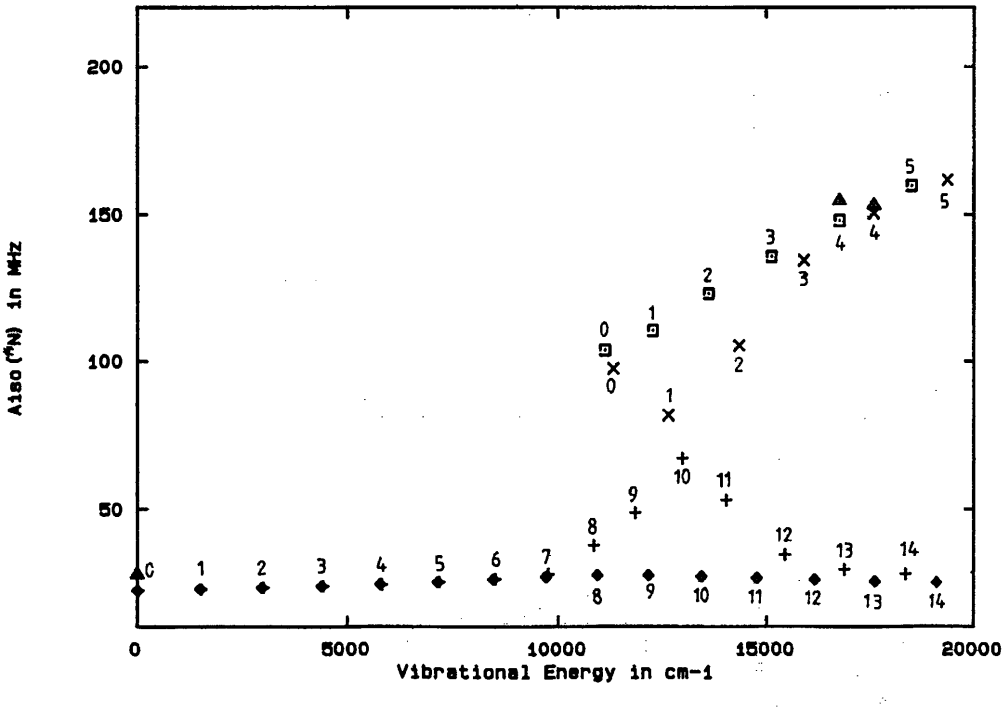

FIG. 10. Vibronically averaged values for $A_{iso}(^{14}\mathrm{N})$ calculated in the present work. The quantum numbers indicate $v_2 = 0$–14 for the $X\,^2B_1$ state and $v_2 = 0$–5 for the $A\,^2A_1$ state; v_1 and v_3 are always zero. ◇ refers to $K = 0$ of the $X\,^2B_1$ state, + refers to $K = 1$ of the $X\,^2B_1$ state, □ refers to $K = 0$ of the $A\,^2A_1$ state, × refers to $K = 1$ of the $A\,^2A_1$ state, and △ refers to experimental values.

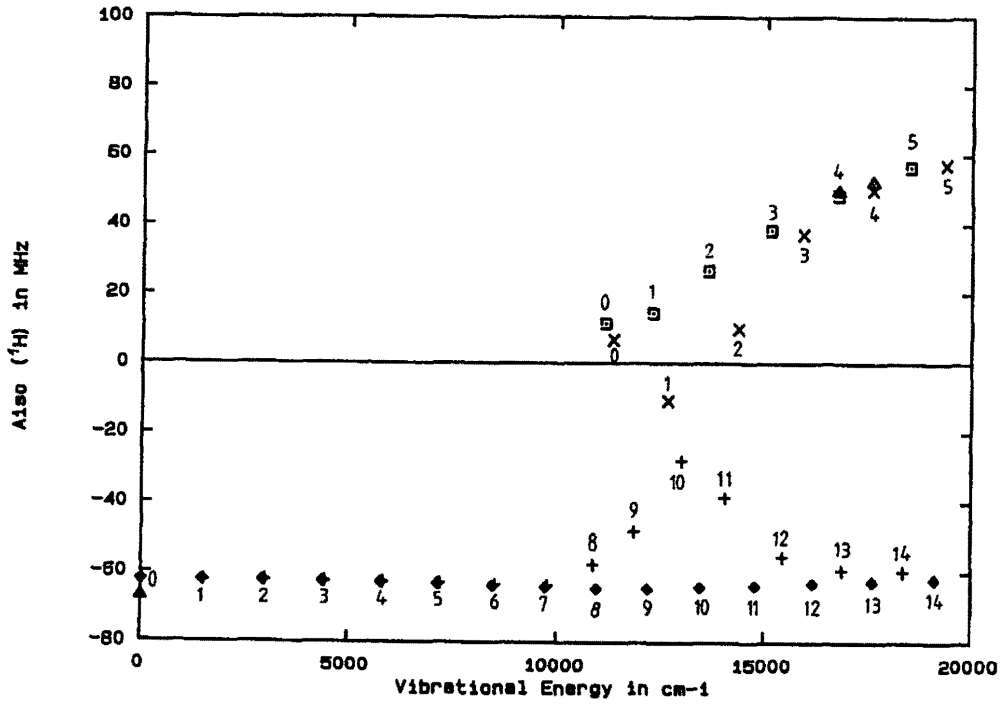

FIG. 11. Vibronically averaged values for A_{iso} (^{1}H). For notations, see Fig. 10.

TABLE II. Mean values of the hyperfine coupling constants (in MHz) at the nitrogen center (^{14}N).

	$K=0$				$K=1$			
v_2[a]	A_{iso}	A_{aa}	A_{bb}	A_{cc}	A_{iso}	A_{aa}	A_{bb}	A_{cc}
				X^2B_1				
0	22	−42	−43	85	22	−42	−43	85
0[b]	28	−43	−45	88				
[c]	± 1	± 2	± 1	± 1				
1	23	−42	−43	85	23	−42	−43	85
2	23	−42	−43	85	23	−42	−43	85
3	24	−42	−43	85	24	−42	−43	85
4	25	−42	−43	85	25	−42	−43	85
5	25	−42	−43	85	25	−42	−43	85
6	26	−42	−43	85	26	−42	−43	85
7	27	−42	−43	85	28	−42	−43	85
8	28	−42	−43	85	38	−42	−43	84
9	28	−42	−43	85	49	−42	−41	84
10	27	−42	−43	85	67	−41	−40	81
11	27	−42	−43	85	53	−41	−41	82
12	26	−42	−43	85	35	−41	−42	84
13	26	−42	−43	85	30	−41	−43	85
14	25	−42	−43	85	28	−42	−43	85
				A^2A_1				
0	104	−40	77	−38	98	−40	77	−38
1	110	−39	77	−38	82	−40	80	−39
2	123	−39	76	−37	105	−39	77	−38
3	136	−38	75	−36	135	−38	75	−37
4	148	−38	74	−36	150	−38	73	−36
4[b]	154	−49			153	−40	76	−37
[d]	± 3	± 5			± 1	± 3	± 1	± 2
5	160	−37	73	−35	162	−37	73	−35

[a] Bending quantum numbers, v_1 and v_3 are always zero.
[b] Experimental values (Ref. 4).
[c] Third standard deviation (Ref. 4).
[d] First standard deviation (Ref. 4).

TABLE III. Mean values of the hyperfine coupling constants (in MHz) at the hydrogen center (^{1}H).

	$K=0$					$K=1$				
v_2[a]	A_{iso}	A_{aa}	A_{bb}	A_{cc}	A_{ab}	A_{iso}	A_{aa}	A_{bb}	A_{cc}	A_{ab}
					X^2B_1					
0	−62	20	−13	−7	55	−62	20	−13	−7	55
0[b]	−67	20	−14	−5	59					
[c]	± 1	± 2	± 2	± 1	± 3					
1	−62	20	−13	−7	54	−62	20	−13	−7	54
2	−62	20	−14	−7	52	−62	20	−13	−7	52
3	−62	20	−14	−6	50	−62	20	−14	−6	50
4	−63	21	−15	−6	49	−63	21	−14	−6	49
5	−63	22	−15	−6	47	−63	21	−15	−6	47
6	−64	23	−17	−6	45	−63	22	−16	−6	45
7	−64	23	−18	−6	42	−64	25	−19	−6	41
8	−65	24	−18	−6	40	−57	34	−28	−6	28
9	−65	23	−17	−6	39	−48	38	−32	−6	21
10	−64	21	−15	−6	39	−28	40	−34	−6	14
11	−64	18	−13	−6	40	−38	29	−23	−6	26
12	−63	16	−10	−5	41	−55	20	−15	−5	36
13	−62	13	−8	−5	41	−59	16	−11	−5	39
14	−62	11	−6	−5	41	−60	13	−8	−5	37
					A^2A_1					
0	12	61	−7	−53	−13	7	53	−7	−46	−5
1	14	60	−7	−53	−14	−11	43	−7	−37	8
2	27	59	−7	−52	−16	10	49	−6	−43	−3
3	38	58	−6	−52	−18	37	54	−6	−48	−15
4	48	56	−5	−51	−20	50	54	−5	−49	−18
4[b]	49	49				52	60	−10	−37	
[d]	± 6	± 11				± 2	± 4	± 2	± 2	
5	57	55	−4	−51	−21	58	53	−4	−49	−19

[a] Bending quantum numbers, v_1 and v_3 are always zero.
[b] Experimental values (Ref. 4).
[c] Third standard deviation (Ref. 4).
[d] First standard deviation (Ref. 4).

ner–Teller interaction is very weak for energetic reasons. Between 10 000 and 16 000 cm^{-1} a strong interaction arises and $A_{iso}(^{14}N)$ averaged for a single vibronic state is heavily modulated due to the admixture of the other electronic state. For vibronic states attributed mainly to the ground state $X\,^2B_1$, $A_{iso}(^{14}N)$ increases sharply from 28 MHz ($v_2 = 7^-$) to 67 MHz ($v_2 = 10^-$). For higher states, the mixing with $A\,^2A_1$ becomes smaller and hence $A_{iso}(^{14}H)$ decreases to 28–29 MHz which is very similar to the value of 25–26 MHz for the corresponding $K = 0$ states. The difference of about 2 MHz shows the small remaining influence of the higher electronic state.

For $K = 1$ states assigned mainly to $A\,^2A_1$, the situation is inverted, because the calculated value of $A_{iso}(^{14}N)$ decreases with increasing $X\,^2B_1$ admixture. For the lowest state $v_2 = 0$, the calculated $A_{iso}(^{14}N)$ value of the $K = 1$ state lies about 6 MHz below the $A_{iso}(^{14}N)$ value of the corresponding $K = 0$ state (98 vs 104 MHz). Due to a stronger $X\,^2B_1$ admixture, the difference increases to about 30 MHz for $v_2 = 1$ with 110 MHz for $K = 0$ vs 82 MHz for $K = 1$. For higher states, the interaction between both electronic states decreases and the values of corresponding vibrational states become very similar. Our results for the $v_2 = 4$, $K = 1$ level of 151 MHz is in very good agreement with the experimental value of 153 MHz ($\pm$ 1.3 MHz in first standard deviation).[4(d)] From the experimental side, no further data are known. From Fig. 10, it can be seen that the calculated values of $A_{iso}(^{14}N)$ for $K = 1$ states lie below the line connecting the $K = 0$ states. Nevertheless, for $v_2 = 4$ and 5, due to the strong dependence of $A_{iso}(^{14}N)$ on the bending angle Θ, $A_{iso}(^{14}N)$ of the $K = 1$ state is higher than the value of the corresponding $K = 0$ state. For $v_2 = 4$, this finding is different from the experimental measurements[4(d)] which place $A_{iso}(^{14}N)$ of $K = 0$ (155 MHz) above $A_{iso}(^{14}N)$ of $K = 1$ (153 MHz). However, due to the large experimental uncertainties, we expect that the theoretical ordering is more reliable. Similar trends as found for $A_{iso}(^{14}N)$ can be seen $A_{iso}(^1H)$ (Fig. 11) and to a smaller extent for the elements of the dipolar tensors summarized in Tables II and III.

Besides the effects arising from vibrational averaging, another interesting aspect appears if the isotropic hyperfine coupling constants of $X\,^2B_1$ and $A\,^2A_1$ are compared. At linear geometry, $X\,^2B_1$ and $A\,^2A_1$ represent the two components of the doubly degenerate $^2\Pi_u$ state and split if the molecule is bent. The electronic configuration of $X\,^2B_1$ is given by $1a_1^2\ 2a_1^2\ 3a_1^2\ 1b_2^2\ 1b_1^1$. Since the singly occupied $1b_1$ which represents a nearly pure nitrogen p orbital possesses a node in the molecular plane, an RHF calculation gives $A_{iso} = 0$ MHz for all centers. Therefore, the values of A_{iso} are determined by spin polarization effects only. In the bent molecule, the first excited state $A\,^2A_1$ is reached formally by the single excitation $3a_1 \rightarrow 1b_1$ resulting in an RHF determinant $1a_1^2\ 2a_1^2\ 3a_1^1\ 1b_2^2\ 1b_1^2$. Because the singly occupied $3a_1$ orbital possesses a nonvanishing value at the positions of the nucleus A_{iso} is expected to be greater than in $X\,^2B_1$, as was found for the PH_2 molecule.[4(d)] The experimental data known for NH_2 show the trend discussed above for the nitrogen center of NH_2. For the hydrogen center a change in sign occurs between $X\,^2B_1$ and $A\,^2A_1$, but contrary to $A_{iso}(^{14}N)$, the magnitude of $A_{iso}(^1H)$ decreases if the experimental data for $v_2 = 4$, $K = 0$ of $A\,^2A_1$ (50 MHz) are compared with the values found for $v_2 = 0$, $K = 0$ of $X\,^2B_1$ ($-$ 67 MHz). From the experimental data, it is impossible to study the extent of the various effects. A breakdown of this unexpected trend is given in Table IV.

If the influence of the vibrational motion is eliminated by comparing $A_{iso}(^1H)$ calculated at the equilibrium structures of the states in question [$X\,^2B_1$—$\Theta = 103°$, $A_{iso}(^1H) = -62$ MHz; $A\,^2A_1$—$\Theta = 144°$, $A_{iso}(^1H) = 12$ MHz], an enhancement of the unexpected trend is found. The main reason for this trend lies in the different equilibrium geometry of both states as can be seen from a comparison of $A_{iso}(^1H)$ of both states calculated at $\Theta = 103°$ ($X\,^2B_1$— $-$ 62 MHz; $A\,^2A_1$—144 MHz). The low value of $A_{iso}(^1H)$ of $A\,^2A_1$ for $\Theta = 144°$ results from the interplay of RHF effects ($+$ 62 MHz) and polarization/correlation effects ($-$ 50 MHz) which cancel each other. For the nitrogen center, a normal trend exists because RHF and polarization/correlation effects have equal sign.

IV. SUMMARY

In the present paper, the hfccs for the $X\,^2B_1$ and the $A\,^2A_1$ states of NH_2 were calculated as a function of the

TABLE IV. A study of various effects influencing A_{iso} at both centers.

		$X\,^2B_1$			$A\,^2A_1$	
		^1H	^{14}N		^1H	^{14}N
Experimental data	($v_2 = 0$)	$-$ 67 MHz	28 MHz	($v_2 = 4$)	50 MHz	155 MHz
The influence of molecular structure[a]						
$\Theta = 144°$		$-$ 66 MHz	31 MHz		12 MHz	104 MHz
$\Theta = 103°$		$-$ 62 MHz	24 MHz		144 MHz	264 MHz
RHF[b]		0 MHz	0 MHz		62 MHz	64 MHz
Polarization and correlation effects[b]		$-$ 66 MHz	24 MHz		$-$ 50 MHz	40 MHz

[a] Equilibrium geometry of $A\,^2A_1$ is $\Theta = 144$ and of $X\,^2B_1$ is 103°.
[b] At the equilibrium structure of the given state.

bond angle Θ. Using the bending potential curves published by Jungen *et al.*,[2] the mean values of the hfccs for the $K = 0$ and 1 levels were computed. All results are in very good agreement with experimental data. Deviations of about 0–5 MHz can be attributed to the strong influence of correlation effects and inaccuracies in the experimental findings. It can be seen clearly that very accurate *ab initio* methods are able to generate reliable predictions. The study shows that the vibrational motion and the Renner–Teller effect has to be taken into account for a quantitative description of hfccs of the vibrational levels. For low-lying vibrational states of the $X\,^2B_1$ ground state, these effects were found to be negligible. The unexpected low value of A_{iso} (^{1}H) for $A\,^2A_1$ at the equilibrium geometry (Θ = 144°) could be attributed to an interplay of RHF effects (+ 62 MHz) and polarization/correlation effects (− 50 MHz) which nearly cancel each other. For the nitrogen center, both contributions possess equal sign so that the value of A_{iso} (^{14}N) for the $A\,^2A_1$ state is three to four times higher than that of the $X\,^2B_1$ ground state.

ACKNOWLEDGMENTS

The services and computer time made available by the Computer Center of the University of Bonn and the Computer Center of the RWTH Aachen have been essential for the present study. Part of this work was financially supported by the Deutsche Forschungsgemeinschaft (DFG) in the framework of the project En 197/2-2 and by the Leibniz Prize. An operating grant of NSERC (Canada) is also gratefully acknowledged.

[1] (a) D. A. Ramsay, J. Chem. Phys. **25**, 188 (1956); (b) K. Dressler and D. A. Ramsay, *ibid.* **27**, 971 (1957); (c) Philos. Trans. R. Soc. A **251**, 553 (1959); (d) J. W. C. Johns, D. A. Ramsay, and S. C. Ross, Can. J. Phys. **54**, 1804 (1976); (e) M. Kroll, J. Chem. Phys. **63**, 319 (1975); **63**, 1803 (1975).

[2] (a) J. A. Pople and H. C. Longuet-Higgins, Mol. Phys. **1**, 372 (1958); (b) R. N. Dixon, Mol. Phys. **9**, 357 (1965); (c) Ch. Jungen, K.-E. J. Hallin, and A. J. Merer, Mol. Phys. **40**, 25 (1980); (d) C. F. Bender and H. F. Schaefer III, J. Chem. Phys. **55**, 4798 (1971); (e) S. Bell and H. F. Schaefer III, *ibid.* **67**, 5173 (1977); (f) R. J. Buenker, M. Perić, S. D. Peyerimhoff, and R. Marian, Mol. Phys. **43**, 987 (1981); (g) M. Perić, S. D. Peyerimhoff, and R. J. Buenker, *ibid.* **49**, 379 (1983).

[3] R. Renner, Z. Phys. **92**, 172 (1934).

[4] (a) G. W. Hills, J. M. Cook, R. F. Curl, Jr., and F. K. Tittel, J. Chem. Phys. **65**, 823 (1976); (b) J. M. Cook, G. W. Hills, and R. F. Curl, Jr., J. Chem. Phys. **67**, 1450 (1977); (c) T. C. Steimle, J. M. Brown, and R. F. Curl, Jr., *ibid.* **73**, 2552 (1980); (d) G. W. Hills, C. R. Brazier, J. M. Brown, J. M. Cook, and R. F. Curl, *ibid.* **76**, 240 (1982); (e) G. W. Hills and J. M. Cook, J. Mol. Spectrosc. **94**, 456 (1982).

[5] (a) W. Meyer, J. Chem. Phys. **51**, 5149 (1969); (b) R. D. Brown and G. R. Williams, Chem. Phys. **3**, 19 (1974); (c) K. Ohta, H. Nakatsuji, K. Hirao, and T. Yonezawa, J. Chem. Phys. **73**, 1770 (1980); (d) H. Sekino and R. Bartlett, *ibid.* **82**, 4225 (1985); (e) M. Pöhlchen, V. Staemmler, and R. Jaquet, Conference of Theoretical Chemistry, Pontresina (1988); (f) K. Funken, B. Engels, S. D. Peyerimhoff, and F. Grein, Chem. Phys. Lett. **172**, 180 (1990).

[6] M. Perić, B. Engels, and S. D. Peyerimhoff, J. Mol. Spectrosc. **150**, 56 (1991); *ibid* **150**, 70 (1991).

[7] (a) F. B. van Duijnefeld, Technical Report RJ 945, IBM Research Laboratory, San Jose; (b) B. Engels and S. D. Peyerimhoff, Mol. Phys. **67**, 583 (1989); (c) M. Frisch, J. A. Pople, and J. S. Binkley, J. Chem. Phys. **80**, 3265 (1984).

[8] (a) R. J. Buenker and S. D. Peyerimhoff, Theor. Chim. Acta **35**, 33 (1974); **39**, 217 (1974); (b) R. J. Buenker, S. D. Peyerimhoff, and W. Butscher, Mol. Phys. **35**, 771 (1978).

[9] M. Perić and B. Engels (in preparation).

[10] M. Perić, S. D. Peyerimhoff, and R. J. Buenker, Int. Rev. Phys. Chem. **4**, 85 (1985).

[11] (a) J. T. Hougen, P. R. Bunker, and J. W. Johns, J. Mol. Spectrosc. **34**, 136 (1970); (b) P. R. Bunker and B. M. Laudsberg, *ibid.* **67**, 374 (1977).

[12] J. D. Graybeal, *Molecular Spectroscopy* (McGraw-Hill, New York, 1988).